Bioorganic Chemistry 91 (2019) 103138

Contents lists available at ScienceDirect

Bioorganic Chemistry

journal homepage: www.elsevier.com/locate/bioorg

Designing of promising medicinal scaffolds for Alzheimer's disease through enzyme inhibition, lead optimization, molecular docking and dynamic simulation approaches

Mubashir Hassan[a,*], Muhammad Athar Abbasi[b,*], Aziz-ur-Rehman[b], Sabahat Zahra Siddiqui[b], Saba Shahzadi[c], Hussain Raza[d], Ghulam Hussain[b], Syed Adnan Ali Shah[e,f], Muhamamd Ashraf[g], Muhammad Shahid[h], Sung-Yum Seo[d], Arif Malik[a]

[a] Institute of Molecular Biology and Biotechnology (IMBB), The University of Lahore, Raiwind Road, 55150 Lahore, Pakistan
[b] Department of Chemistry, Government College University, Lahore 54000, Pakistan
[c] Institute of Molecular Science and Bioinformatics, Nisbat Road, Lahore, Pakistan
[d] College of Natural Science, Department of Biological Sciences, Kongju National University, Gongju 32588, South Korea
[e] Faculty of Pharmacy, Universiti Teknologi MARA, Puncak Alam Campus, 42300 Bandar Puncak Alam, Selangor Darul Ehsan, Malaysia
[f] Atta-ur-Rahman Institute for Natural Products Discovery (AuRIns), Level 9, FF3, Universiti Teknologi MARA, Puncak Alam Campus, 42300 Bandar Puncak Alam, Selangor Darul Ehsan, Malaysia
[g] Department of Chemistry, The Islamia University of Bahawalpur, Bahawalpur 63100, Pakistan
[h] Department of Biochemistry, University of Agriculture, Faisalabad 38040, Pakistan

ARTICLE INFO

Keywords:
Piperazine
Sulfonamide
Enzyme inhibition
Hemolysis
Molecular docking
Dynamic simulation

ABSTRACT

In the designed research work, a series of 2-furoyl piperazine based sulfonamide derivatives were synthesized as therapeutic agents to target the Alzheimer's disease. The structures of the newly synthesized compounds were characterized through spectral analysis and their inhibitory potential was evaluated against butyrylcholinesterase (BChE). The cytotoxicity of these sulfonamides was also ascertained through hemolysis of bovine red blood cells. Furthermore, compounds were inspected by Lipinki Rule and their binding profiles against BChE were discerned by molecular docking. The protein fluctuations in docking complexes were recognized by dynamic simulation. From our *in vitro* and *in silico* results **5c**, **5j** and **5k** were identified as promising lead compounds for the treatment of targeted disease.

1. Introduction

Sulfonamides are antibacterial agents, but their uses have proven to treat some other diseases [1]. Sulfonamides are also have also been reported to exhibit inhibitory activities against various enzymes including carbonic anhydrase, cysteine protease, HIV protease, cyclooxygenase [2] and acetylcholinesterase and butyrylcholinestearse (BChE) [3-7]. The piperazine derivatives have been shown to inhibit human acetylcholinesterase [8]. The previous research showed that presence of benzyl piperidine/piperazine and benzhydrylpiperazine moiety in AChE inhibitors (AChEIs) mainly contribute to inhibitory activity by interacting with the active site of AChE and has also been efficiently used for design AChEIs [9].

BChE is an important target for Alzheimer's disease (AD) treatment [10]. The expression study showed that BChE is expressed in the hippocampus and temporal neocortex regions of human brain [11]. The invitro analysis showed that BChE can be associated with amyloid-β (Aβ) protein and may delay the onset and rate of neurotoxic Aβ fibril formation [12]. AD is characterized by marked cholinergic dysfunction [13,14]. More specifically, degeneration of cholinergic neurons; loss of cholinergic transmission; depletion of ACh, especially in moderate-to-severe disease stages; and changes in AChE and BuChE activity are commonly observed in the cerebral cortex and hippocampus of patients with AD [14,15].

Organic chemists and pharmacists have keen interest to synthesize or design new therapeutically important drug constituents to treat AD. Therefore, in the present research, a new series of chemical compounds were synthesized and evaluated using *in vitro* and *in silico* approaches. All these compounds were screened for their possible enzyme inhibitory potential and their hemolytic activity was also tested to find their utility as possible therapeutic agent. Furthermore, lead optimization, pharmacokinetics and cheminformatics analyses were implemented to check

* Corresponding authors.
E-mail addresses: mubashirhassan_gcul@yahoo.com, mubasher.hassan@imbb.uol.edu.pk (M. Hassan), abbasi@gcu.edu.pk (M.A. Abbasi).

https://doi.org/10.1016/j.bioorg.2019.103138
Received 31 May 2019; Received in revised form 8 July 2019; Accepted 19 July 2019
Available online 22 July 2019

their biochemical properties and Lipinski Rule (RO5) validation. Molecular docking and dynamic simulation techniques were used to check their binding affinity against target protein and stability behavior of docked structures by Root Mean Square Deviation and Fluctuations (RMSD/RMSF) graphs.

The aim of this study is to investigate the effect of newly sulfonamides based derivatives and their inhibition effect against cholinesterase. Based on our *in vitro* and *in silico* results, three compounds can serve as appropriate chemical scaffolds for the designing of new medicinal compounds for the treatment of Alzheimer's disease.

2. Experimental data

2.1. General

Chemicals were purchased from Sigma Aldrich and Alfa Aesar (Germany) and solvents of analytical grade were supplied by local suppliers. By using an open capillary tube method melting point of all the synthesized compounds were taken on Griffin and George melting point apparatus and were uncorrected. By using thin layer chromatography (with various percentages of ethyl acetate & *n*-hexane as mobile phase), the purity of the synthesized compounds was detected at 254 nm. IR peaks were recorded on a Jasco-320-A spectrophotometer by using a KBr pellet method. ^{1}H NMR signals were recorded at 600 MHz and ^{13}C NMR at 150 MHz in $CDCl_3$ using Bruker spectrometers. EIMS signals were recorded by utilizing a JMS-HX-110 spectrometer.

2.2. Synthesis of 2{4-[(3,5-Dichloro-2-hydroxyphenyl)sulfonyl]-1-piperazinyl}(2-furyl)methanone (3)

2-Furyl(1-piperazinyl)methanone (12.8 mmol; 2.31 g, **1**) was suspended in 100 mL water and the pH was maintained at 9.0–10.0 by adding an aqueous solution of 10% Na_2CO_3 followed by slow addition of 3,5-dichloro-2-hydroxybenzenesulfonyl chloride (12.8 mmol; 3.55 g, **2**) to the reaction mixture over 10–15 min. The reaction mixture was stirred at RT for 3 h and monitored with TLC till completion of the reaction. Conc. HCl (around 4 mL) was then added slowly to adjust the pH to 2.0 and reaction medium was rested at RT for 15 min, light brown amorphous solid was filtered and washed with distilled water to afford {4-[(3,5-dichloro-2-hydroxyphenyl)sulfonyl]-1-piperazinyl}(2-furyl) methanone (**3**) after drying.

2.3. Synthesis of {4-[(2-Alkoxy/aralkyloxy-3,5-dichlorophenyl)sulfonyl]-1-piperazinyl}(2-furyl)methanones (5a–l)

{4-[(3,5-Dichloro-2-hydroxyphenyl)sulfonyl]-1-piperazinyl}(2-furyl)methanone (1.66 mmol; 0.2 g, **3**) in *N,N*-dimethylformamide (5 mL) and catalytic amount of lithium hydride (0.42 mmol, 0.01 g) was added in a 25 mL round bottomed flask and stirred for 15 min at room temperature after which corresponding alkyl/aralkyl halides (1.66 mmol; **4a–l**) were added in the reaction mixture which was further stirred for 4–5 hrs. After reaction completion, reaction mixture was quenched with ice cold water (200 mL). The obtained solid was filtered, washed with distilled water and dried to yield the corresponding {4-[(2-alkoxy/aralkyloxy-3,5-dichlorophenyl)sulfonyl]-1-piperazinyl}(2-furyl)methanones (**5a–l**). In some cases, the compound was isolated via solvent extraction using chloroform/ethyl acetate as organic solvent. The spectral characterization of the synthesized compounds is given in supplementary data.

2.4. BChE inhibition assay

Newly synthesized compounds were tested against horse serum BChE. In vitro inhibition potencies of synthesized derivatives were determined by spectrophotometric method established by Ellman [16] with little modifications. A mixture consisting of 60 µL phosphate buffer (KH2PO4/ KOH, having pH 7.7), a 10 µL test compounds (end concentration of DMSO was 1%) and 10 µL enzyme (0.015 unit/ well for BChE (horse serum). The mixture was incubated at 37 °C for 10 min for pre incubation. After this, 10 µL substrate (butyrylthiocholine chloride, 1 mM) were added to respective BChE reaction mixtures to start the reaction. Later, 10 µL of 0.5 mM DTNB was added as coloring reagent. After this incubation at 37 °C for 20 min was carried out and later on measurements were taken at 405 nm with plate reader (Bio-Tek ELx 800TM, USA). All the experiments were carried out in triplicate and the results were calculated as percentage inhibition values. The compounds which exhibited above 50% inhibition against cholinesterase were further checked by 7–8 dilutions to get the IC_{50} values by GraphPad PRISM (USA). Eserine was used as a standard to compare our results. Percent inhibitions calculated by the following formula:

$$\text{Inhibition}(\%) = \frac{Control - Test}{Control} \times 100$$

2.5. Statistical analysis

The results are written as mean ± SEM after performance in threefolds and statistical analysis by Microsoft Excel 2010.

2.6. Hemolytic activity

Hemolytic activity was done by the reported method [17,18]. Bovine blood was obtained from Department of Clinical Medicine and Surgery, University of Agriculture, Faisalabad, Pakistan. After centrifugation, separation and washing, the % RBCs lysis was computed by noting the absorbance.

2.7. Computational methodology

2.7.1. Repossession of BChE from PDB

The three dimensional (3D) crystal structure of BChE in complex with tacrine with PDBIDs 4BDS was accessed from Protein Data Bank (PDB) (www.rcsb.org) [19]. The target protein structure was refined by removing unnecessary ligands and protein structure was further minimized with amber force field by using conjugate gradient algorithm in UCSF Chimera 1.6rc [20]. The protein architecture and statistical their percentage values of α-helices, β-sheets, coils and turns were calculated from online VADAR 1.8 server [21]. The Discovery Studio R2 Client a visualizing tool was used to generate the hydrophobicity graph. The protein Ramachandran graph was accessed through PDB. The Discovery Studio R2 Client [22] was used to view 3D structure of target proteins.

2.7.2. Designing of ligands in ACD/ChemSketch

The synthesized ligands (**5a–l**) were sketched in ACD/ChemSketch and accessed in mol format. The biochemical properties and Lipinski's rule of five (RO5) of synthesized compounds (**5a–l**) were evaluated and justified using online computational tools such as Molinspiration (http://www.molinspiration.com/) and Molsoft (http://www.molsoft.com/), respectively. The bioactivity scores prediction of all synthesized compounds was also generated by Molinspiration. Moreover, the pharmacokinetic properties like Absorption, Distribution, Metabolism, Excretion and Toxicity (ADMET) were evaluated through pkCSM online server [23]. Furthermore, ligand efficacy was determined by Dataworrior tool [24].

2.7.3. Molecular docking simulation

Based on in-vitro results **5c, 5j** and **5k** were selected to check the binding configurations against target protein. Molecular docking experiment was carried out on synthesized ligand (**5c, 5j** and **5k**) against BChE using PyRx (VINA Wizard) docking tool. In detail docking experiment all the synthesized chemical structures were sketched in ACD/

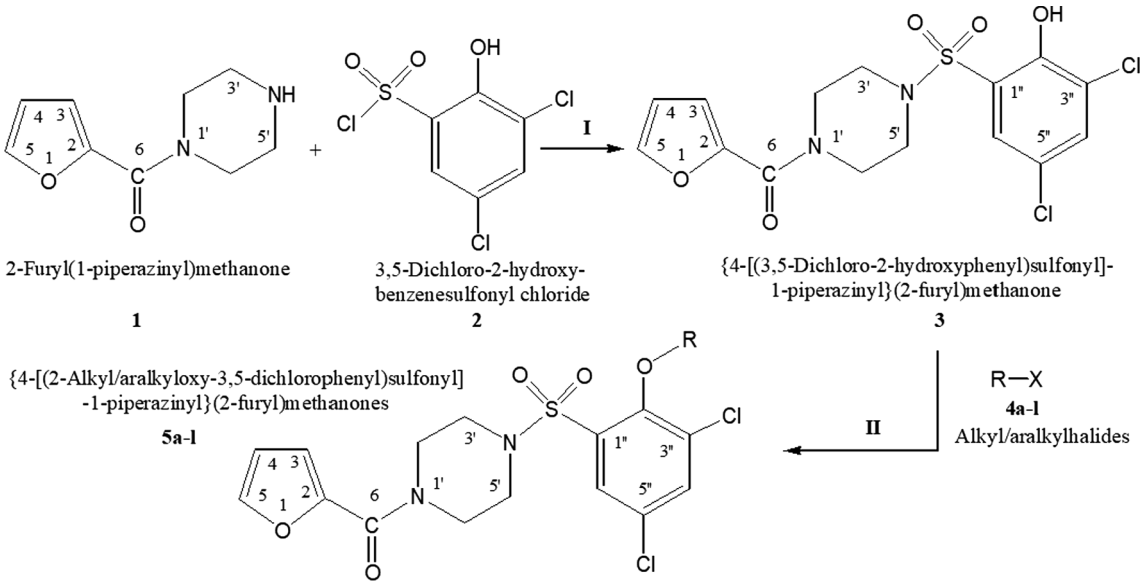

Fig. 1. Schematic outline for the synthesis of {4-[(2-alkoxy/aralkyloxy-3,5-dichlorophenyl)sulfonyl]-1-piperazinyl}(2-furyl)methanones. Different derivatives are shown in this figure. Reagents & Conditions: (I) Aq. 10% Na_2CO_3 soln./pH 9–10/stirring at RT for 3 hrs. (II) DMF/LiH/stirring for 4–5 h.

ChemSketch tool and accessed in mol format. Furthermore, UCSF Chimera 1.6rc tool was employed to energy minimization of each ligand separately having default parameters such as steepest descent steps 100 with step size 0.02 (Å), conjugate gradient steps 100 with step size 0.02 (Å) and update interval was fixed at 10. Finally, Gasteiger charges were added using Dock Prep in ligand structure to obtain the good structure conformation. Molecular docking experiment was employed on all the ligands, **5a–l**, against Jack bean urease by using virtual screening tool PyRx with VINA Wizard approach [25]. The grid box parameters values in VINA search space (X = 30.1117, Y = −53.4363 and Z = 57.7440) were adjusted with default exhaustiveness value = 8 to maximize the binding conformational analysis. For better prediction of ligand conformation, we have adjusted sufficient grid box size on biding pocket residues to allow the ligands to move freely in the search space. All the synthesized ligands were docked separately against target protein. In all docked complexes, the ligands conformational poses were keenly observed to obtain the best docking results. The generated docked complexes were evaluated on the basis of lowest binding energy (kcal/mol) values and binding interaction pattern between ligands and receptor. The graphical depictions of all the docked complexes were accomplished by UCSF Chimera 1.6rc and Discovery Studio R2 Client, respectively.

2.7.4. Molecular dynamics (MD) simulations

To understand the residual backbone flexibility of protein structure, MD simulations were carried out by Groningen Machine for Chemicals Simulations (GROMACS 4.5.4 package [26], with GROMOS 96 force field [27]. The overall system charge was neutralized by adding ions. The steepest descent approach (1000 ps) for protein structure was applied for energy minimization. For energy minimization the nsteps = 50,000 were adjusted with energy step size (emstep) 0.01 value. Particle Mesh Ewald (PME) method was employed for energy calculation and for electrostatic and van der waals interactions; cut-off distance for the short-range VdW (rvdw) was set to 14 Å, whereas neighbour list (rlist) and nstlist values were adjusted as 1.0 and 10, respectively, in em.mdp file [28]. It permits the use of the Ewald summation at a computational cost comparable with that of a simple truncation method of 10 Å or less, and the linear constraint solver (LINCS) [29] algorithm was used for covalent bond constraints and the time step was set to 0.002 ps. Finally, the molecular dynamics simulation was carried out at 20,000 ps with nsteps 10,000,000 in md.mdp file. Different structural evaluations such as root mean square deviations and fluctuations (RMSD/RMSF), solvent accessible surface areas (SASA) and radii of gyration (Rg) of back bone residues were analysed through Xmgrace software (http://plasma-gate.weizmann.ac.il/Grace/) and UCSF Chimera 1.10.1 software.

3. Results and discussion

The aim of the present research work was to synthesize some new molecules having suitable therapeutic potential. With this point of view, some new piperazine containing sulfonamides were synthesized and evaluated though *in vitro* assay against butyrylcholinestearse followed by computational approaches.

3.1. Chemistry

The synthesis was initiated by the coupling of 2-furyl(1-piperazinyl) methanone (2-fuoroyl-1-piperazine; **1**) with 3,5-dichloro-2-hydroxybenzenesulfonyl chloride (**2**) under dynamic pH control in aqueous medium [30] to acquire the parent compound, {4-[(3,5-dichloro-2-hydroxyphenyl)sulfonyl]-1-piperazinyl}(2-furyl)methanone (**3**). Further, the reaction of **3** with different alkyl/aralkyl halides (**4a–l;** Fig. 1) yielded a series of {4-[(2-alkoxy/aralkyloxy-3,5-dichlorophenyl)sulfonyl]-1-piperazinyl}(2-furyl)methanones (**5a–l**) as outlined in (Fig. 1). The structures of different derivatives are shown in Fig. 1. The synthesis of all these derivatives was performed in DMF (*N*,*N*-dimethylformamide) and lithium hydride (LiH) as a base. The products were isolated by adding ice cold water in the reaction mixture and then filtering off the precipitated solid. In some cases, compounds were taken out through solvent extraction method using chloroform as organic phase. The structures of these molecules were confirmed through spectral data as described in experimental section. The designed synthesized structures of different derivatives have been shown in (Fig. 2).

3.2. BChE inhibition and structure-activity relationships

The synthesized sulfonamides (**5a–l**) were evaluated for their inhibitory potentials against BChE enzymes and the results are tabulated in Table 1. A varying degree of inhibition was displayed by these sulfonamides ranging from 9.51 ± 0.06 to 86.12 ± 0.13 μM against this enzyme, when compared with highly potent standard inhibitor eserine

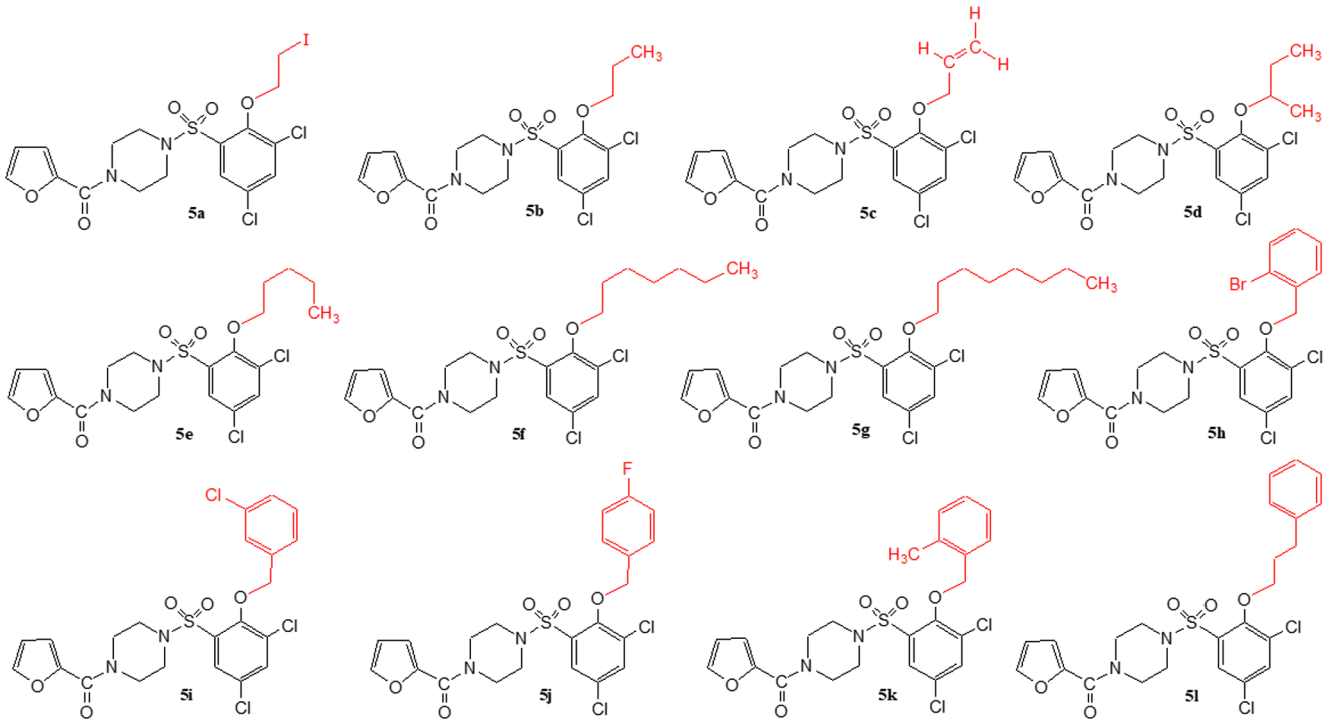

Fig. 2. Structures of different derivatives, **5a–5l**.

having IC_{50} value of 0.85 ± 0.01 μM. Some of the molecules, for example, **5c**, **5k,** and **5j**, exhibited noteworthy inhibitory potentials with IC_{50} values of 9.51 ± 0.06, 15.43 ± 0.09, and 17.69 ± 0.07 μM, respectively, against this enzyme.

Though the exposed activity is accumulative of a whole molecule, yet a limited structure-activity relationship (SAR) was recognized by examining the effect of different alkyl or aralkyl entity on the inhibitory potential, as it was the only varying part and all other parts were same in all molecules. The general structural parts of the studied sulfonamides are featured in (Fig. 3).

When the inhibitory potential of compounds having two to three-carbon chain on oxygen atom, was compared, it was revealed that **5c** bearing an unsaturated chain (allyloxy group) behaved as a superb inhibitor with an IC_{50} value of 9.51 ± 0.06 μM. The saturation of same three-carbon chain (propxy group) in **5b** resulted in a decrease of inhibitory activity (IC_{50} = 82.02 ± 0.09 μM) and even a further decrease in activity of **5a** (IC_{50} = 85.62 ± 0.15 μM) was observed when a bulky iodo group was present at terminal position (Fig. 4). In fact, the molecule **5c** was the most active compound in the synthetic series. It means that this molecule with a small and unsaturated group probably interacted with the active site of the enzyme in a best suitable manner.

On comparison of inhibitory potential of following four molecules, it was lucid that either branching of chain as in **5d** or lengthening of chain as in **5e** to **5g** were not rendering any encouraging activity to these molecules, probably due to steric reasons (Fig. 5).

The compounds **5h** and **5k** both were having an *ortho* substituent on the aralkyloxy part, however, the former was bearing a bulky bromo group while the latter contained a small methyl group (Fig. 6). From their bioactivity, it was clear that the latter molecule exhibited much better potential (IC_{50} = 15.43 ± 0.09 μM) as compared to the former molecule (IC_{50} = 34.52 ± 0.08 μM). It means, the presence of a small sized group on benzyloxy part attributed the molecule to have splendid interactions with the enzyme. The molecule **5 k** was also identified as the second most active compound among the synthetic derivatives.

Among the following derivatives, the compound **5i** had a medium-sized chloro group, **5j** was having again a small size fluoro group while there was a three-carbon chain in between phenyl ring and oxygen atom in **5l** (Fig. 7). From their inhibitory data, it was discernible that the insertion of chain in **5l** retarded its activity significantly and it was the least active compound in the series. However, the presence of a small fluoro group in **5j** attributed this compound with a suitable

Table 1
BChE enzyme inhibition studies of active {4-[(2-alkyl/aralkyloxy-3,5-dichlorophenyl)sulfonyl]-1-piperazinyl}(2-furyl)methanones.

Compounds	Inhibition (%)	IC_{50} (μM)
5a	71.35 ± 0.32	85.62 ± 0.15
5b	68.43 ± 0.32	82.02 ± 0.09
5c	92.41 ± 0.32	9.51 ± 0.06
5d	81.67 ± 0.31	47.85 ± 0.23
5e	73.22 ± 0.23	64.21 ± 0.15
5f	71.36 ± 0.28	75.62 ± 0.13
5g	76.29 ± 0.36	52.94 ± 0.17
5h	82.63 ± 0.23	34.52 ± 0.08
5i	78.85 ± 0.25	43.75 ± 0.11
5j	85.77 ± 0.24	17.69 ± 0.07
5k	88.28 ± 0.31	15.43 ± 0.09
5l	75.32 ± 0.21	86.12 ± 0.13
Eserine	**82.82 ± 1.09**	**0.85 ± 0.0001**

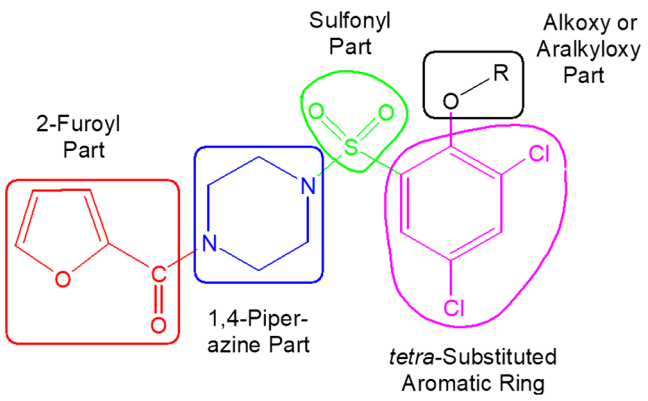

Fig. 3. General structural features of compounds **5a–l**.

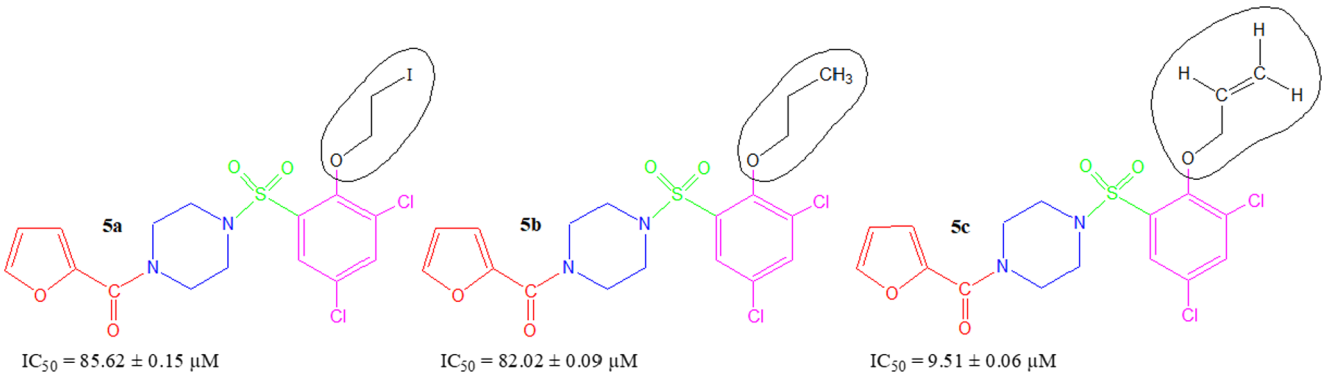

Fig. 4. Structure-activity relationship of compounds **5a**, **5b**, and **5c**.

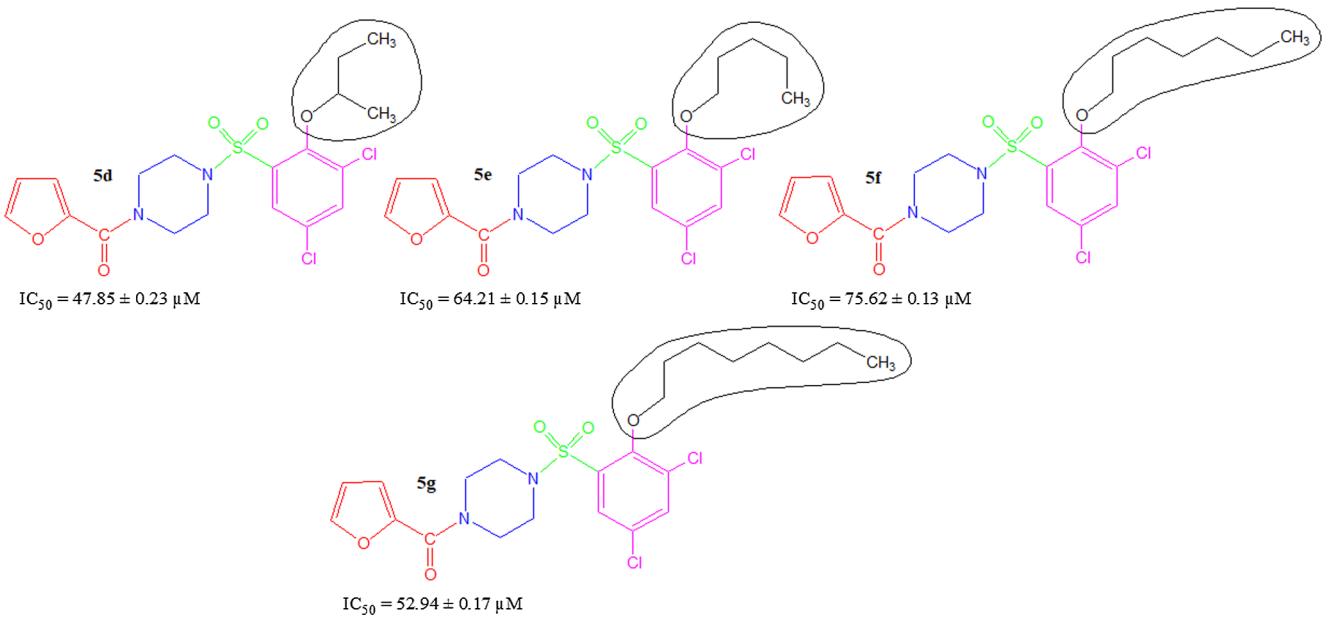

Fig. 5. Structure-activity relationship of compounds **5d**, **5e**, **5f**, and **5g**.

activity (IC_{50} = 17.69 ± 0.07 µM), relative to **5i** in which a relatively bulky group was present (IC_{50} = 43.75 ± 0.11 µM).

So, it was obvious from the structure-activity relationship that among the designed derivatives, compounds with small sized unsaturated alkoxy as well as less bulky aralkyloxgy groups are good inhibitors of this enzyme.

3.3. Hemolytic activity

All the synthesized molecules were evaluated for their cytotoxicity profile through their hemolytic study and % lysis of RBCs is given in Table 2. The hemolytic results showed that few compounds **5b**, **5c**, **5g** and **5k** exhibited good hemolytic activity having 6.69, 6.31, 5.56 and 6.69%, respectively. On the basis of these results, it can be inferred that these synthesized molecules might be utilized as potent therapeutic

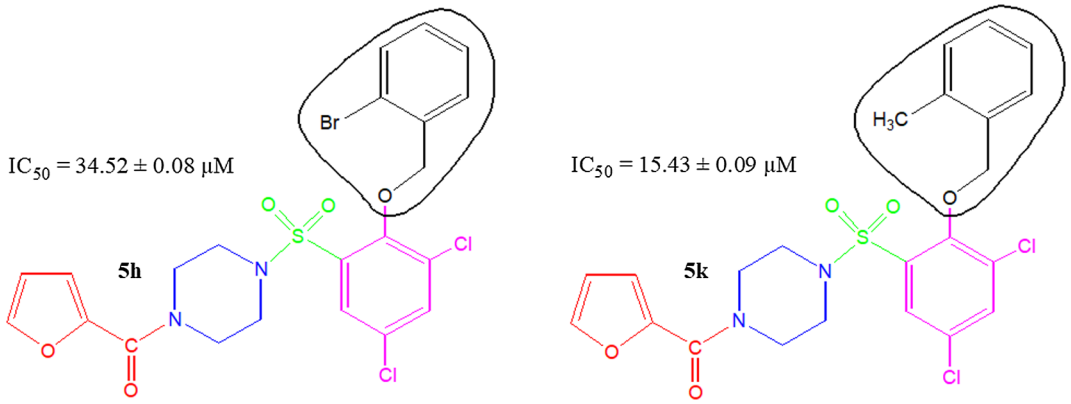

Fig. 6. Structure-activity relationship of compounds **5h**, and **5k**.

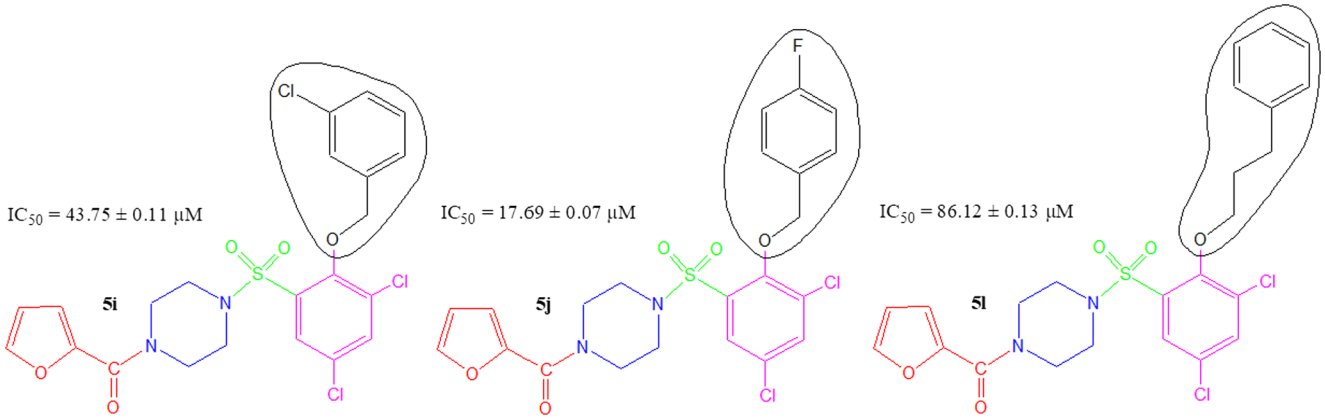

Fig. 7. Structure-activity relationship of compounds **5i**, **5j**, and **5l**.

Table 2
Hemolytic activity of synthetic compounds (**5a–l**).

Compounds	Hemolytic activity(%)	Compounds	Hemolytic activity(%)
5a	34.72	**5h**	15.89
5b	6.69	**5i**	30.92
5c	6.31	**5j**	39.74
5d	30.54	**5k**	6.69
5e	35.14	**5l**	71.92
5f	27.61	**Triton**	89.11
5g	5.56	**PBS**	0.09

entrants for certain ailments.

3.4. Computational analysis

3.4.1. Structural assessment of BChE

Human BChE is a class of hydrolase protein having single chain (A) comprises 529 amino acids. The VADAR 1.8 structure analysis of human BChE consists of 34% α-helices, 23% β-sheets, 41% coils and 25% turns, respectively. The Ramachandran plots and values of BChE indicated that 96. 1% of protein amino acids were present in favored region and 99.6% residues were lie in allowed region. The Ramachandran graph values showed the good accuracy of phi (φ) and psi (ψ) angles among the coordinates of receptor and most of residues were plunged in acceptable region. The Ramachandran and hydrophobicity graphs of target structure is mentioned in supplementary data (Fig. S1A, B), respectively.

3.4.2. Bio-chemical properties and Lipinski's rule of five (RO5) validation

The biochemical properties of all the synthesized compounds (**5a–l**) were predicted by using computational tools. The synthesized compounds (**5a–l**) were validated through RO5 analysis. It has been observed that molecular mass and log*P* values less than 500 (g/mol) and 5, respectively. Moreover, the compounds should possess no greater than 10 HBA and 5 HBD, respectively. The molecular weight (g/mol) of most of most compounds **5a**, **5f–5l** were exceeded then standard value (Table 3). The exceed values of HBA and HBD results in poor permeation [27]. The hydrogen-bonding capacity has been considered as significant parameter for drug permeability. Our results justified that the all synthesized compounds possess < 10 HBA and < 5 HBD values which were comparable with standard values. However, log*P* values for most of compounds were also comparable with standard value (> 5) except **5f–5i** and **5l**. However, multiple examples are available for RO5 violation amongst the existing drugs [32,33].

The number of rotatable bonds within chemical structures is also a significant topological parameter to measure the molecular flexibility. It has been shown to be a very good descriptor for oral bioavailability of drugs [30]. Rotatable bonds can be defined as any single non-ring bond, bounded to nonterminal heavy (i.e., non-hydrogen) atom. However, amide C—N bonds are not considered as rotatable bond due to their high rotational energy barrier. Prior research showed that increased number of rotatable bonds (≥10) has been associated with poor oral bioavailability, particularly when associated with a high polar surface area (> 140 Å2) [25]. Our predicted results justify that all compounds exhibited < 10 rotatable bonds which ensured the significance of our chemical compounds have some drug like behavior. Polar surface area (PSA) is also considered as good descriptor for characterizing the drug absorption, including intestinal absorption, bioavailability and blood-brain barrier penetration. Our predicted results showed that all compounds possess < 140 $Å^2$ PSA values.

Drug-likeness is amalgam of complex balance of various molecular properties such as hydrophobicity, electronic distribution, hydrogen bonding characteristics, molecule size and flexibility and presence of various pharmacophoric features [34]. Our results showed that all the

Table 3
Biological properties of synthesized compounds.

Ligands	Mol.weight (g/mol)	No. HBA	No. HBD	Rotatable Bonds	Mol. Log*P*	MolPSA (A^2)	Mol. Vol (A^3)	Drug likeness Score
5a	557	6	0	6	3.67	64.57	389.40	1.17
5b	446	6	0	6	3.82	64.57	390.96	1.25
5c	444	6	0	6	3.61	64.57	394.64	0.85
5d	460	6	0	6	4.18	63.84	406.17	1.51
5e	478	6	0	6	4.79	64.84	426.78	0.88
5f	502	6	0	10	5.75	64.57	462.59	0.88
5g	516	6	0	11	6.23	64.57	480.50	0.87
5h	571	6	0	6	5.21	64.38	448.48	0.63
5i	528	6	0	6	5.19	64.38	444.39	1.10
5j	512	6	0	6	4.75	64.38	433.04	1.00
5k	508	6	0	6	4.76	64.38	447.15	0.78
5l	527	6	0	8	5.27	64.30	462.90	1.16

Table 4
Biological properties of synthesized compounds.

Ligands	GPCR ligand	Ion channel modulator	Kinase inhibitor	Nuclear receptor ligand	Protease inhibitor
5a	−0.27	−0.74	−0.65	−0.58	−0.38
5b	−0.24	−0.67	−0.54	−0.47	−0.29
5c	−0.37	−0.73	−0.60	−0.50	−0.38
5d	−0.23	−0.73	−0.65	−0.42	−0.29
5e	−0.17	−0.60	−0.48	−0.41	−0.23
5f	−0.16	−0.56	−0.45	−0.38	−0.21
5g	−0.16	−0.55	−0.44	−0.37	−0.21
5h	−0.28	−0.59	−0.47	−0.48	−0.29
5i	−0.17	−0.52	−0.42	−0.42	−0.20
5j	−0.17	−0.53	−0.39	−0.39	−0.21
5k	−0.20	−0.58	−0.46	−0.41	−0.25
5l	−0.11	−0.49	−0.40	−0.33	−0.16

synthetic compounds (**5a–l**) showed good drug score values. All the compounds showed positive predicted values which depicted good drug likeness behavior (Table 3).

3.4.3. Bioactivity scores prediction

The prediction of bioactivity scores for all synthesized compounds against drug targets were evaluated by Molinspiration (Table 4). Prior report showed some standard range for the compounds to predict their activity. Molecules which possessed > 0.00 bioactivity score are considered as good leads structures exhibited considerable biological activities. Whereas, compounds having bioactivity values range from −0.50 to 0.00 are anticipated as abstemiously active and others contain < −0.50 score are supposed to be inactive [35]. The predicted results clearly reveal that the designed sulfonamides containing piperazine derivatives might be involved in moderate interaction with all drug targets like G-protein-coupled receptors (GPCR) and protease. However, against other receptors such as ion channel modulator, kinases and nuclear receptor the activity prediction was not in the standard range.

3.4.4. Pharmacokinetic assessment of synthesized compounds

The pharmacokinetics/ADMET properties such as absorption, distribution, metabolism, excretion and toxicity of newly synthesized ligands are considered as major hallmark to predict the lead structures efficacy. The absorption properties like water absorption (log mol/L), intestinal solubility (% absorbed) and skin permeability (logKp) values predict the therapeutic potential of newly synthesized compounds. The absorption of drug is depends upon routes of administration either orally, intravenously or subcutaneously. Usually the chemical compounds target a specific tissue by using bloodstream pathway. Absorption critically determines the compound's bioavailability. However, multiple factors including poor compound solubility, gastric emptying time, intestinal transit time, chemical instability in the stomach, and inability to permeate the intestinal wall can all reduce the extent to which a drug is absorbed after oral administration. Prior research data showed that ligands having good absorption value have more chance to cross gut barrier by passive penetration [23]. The water solubility results justified that compounds **5a–l** showed good absorption and may have potential to cross gut barriers. Furthermore, all compounds (**5a–l**) exhibited good intestinal solubility results which are comparable to standard value (> 30 %abs). The skin permeability values of all chemical compounds (**5a–l**) were also present in the acceptable range compared with standard value (−82.5 logKp) which predict their drug likeness behavior. The compounds having < 30% absorption may not considered as good lead like structure. Moreover, Blood Brain Barrier (BBB) and Central Nervous System (CNS) permeability values of all compounds were also acceptable with the standard values (> 0.3 to < −1 log BB and > −2 to < −3 logPS), respectively. Results showed that compounds displayed a comparable predicted values with standard and have potential to cross the barriers and to target the receptor. Moreover, their metabolic behavior was confirmed by CYP1A2, CYP2C19 and CYP2C9 inhibitor, which are isoform of cytochrome P450. Ligands results showed the good inhibitory behavior for CYP2C19 and CYP2C9, however, for CYP1A2 compounds did not show inhibition behavior. The excretion and toxicity predicted values were also justified the drug likeness behavior of these compounds on the basis of total clearance (log ml/min/kg), AMES toxicity, maximum tolerated dose (MTD) and LD_{50} values. The Ames test is one of the most frequently applied tests in toxicology and to check whether a given chemical can cause mutations in the DNA of the test organism [36]. The non-mutagenic and non-toxic behavior was also observed from AMES toxicity prediction. All compounds showed negative results in AMES toxicity prediction. The positive hepatotoxicity behavior showed toxic and sensitive effects of ligands. Compounds showed hepatotoxic behavior while no one showed skin sensitization effects. The predicted ADMET properties justified that these novel synthesized compounds may have good lead like potential with mild hepatotoxic effects (Table 5).

3.4.5. Lead optimization and mutagenic risk assessment

To evaluate the lead optimization behavior of synthesized compounds, DataWarrior tool was used to predict ligand efficiency (LE), lipophilic ligand efficiency (LLE) and lipophilicity-corrected ligand

Table 5
Pharmacokinetic assessment of synthesized compounds (**5a–l**).

ADMET Properties		5a	5b	5c	5d	5e	5f	5g	5h	5i	5j	5k	5l
Absorption	WS	−5.09	−4.86	−4.77	−5.19	−5.29	−5.82	−6.08	−5.83	−5.68	−5.13	−5.63	−6.14
	IS	92.78	93.06	93.53	92.16	91.72	90.82	90.47	91.60	92.67	93.12	93.13	93.01
	SP	−2.90	−3.24	−3.24	−3.28	−3.10	−2.96	−2.90	−2.80	−2.80	−2.76	−2.81	−2.79
Distribution	BBBP	−1.36	−1.18	−1.17	−1.18	−1.23	−1.27	−1.29	−1.37	−1.37	−1.40	−1.19	−1.23
	CNSP	−3.07	−3.04	−3.04	−3.01	−3.01	−2.47	−2.45	−2.25	−2.27	−2.45	−2.32	−2.4
Metabolism (inhibitor)	CYP1A2	No	No	No	No	No	No	No	No	No	No	No	No
	CYP2C19	Yes	Yes	Yes	Yes	Yes	Yes	Yes	Yes	Yes	Yes	Yes	Yes
	CYP2C9	Yes	Yes	Yes	Yes	Yes	Yes	Yes	Yes	Yes	Yes	Yes	Yes
Excretion	TC	0.43	0.45	0.41	0.40	0.52	0.52	0.61	0.22	0.13	0.11	0.15	0.33
Toxicity	AMES	No	No	No	No	No	No	No	No	No	No	No	No
	MTD	0.34	0.39	0.40	0.34	0.48	0.55	0.56	0.25	0.24	0.38	0.25	0.39
	ORAT	2.66	3.17	3.14	3.14	3.12	3.04	3.01	2.92	2.84	2.91	2.86	2.74
	HT	Yes	Yes	Yes	Yes	Yes	Yes	Yes	Yes	Yes	Yes	Yes	Yes
	SS	No	No	No	No	No	No	No	No	No	No	No	No

*__Abbreviation__: WS = Water solubility (log mol/L), IS = intestinal solubility (%abs), SP = Skin permeability (log Kp), BBBP = blood brain barrier permeability (Log BB), CNSP = CNS permeability (LogPS), TC = Total clearance (log ml/min/kg), MTD = Max. tolerat. dose ORAT = Oral Rat Acute Toxicity (LD_{50}), HT = Hepatotoxicity, SS = Skin Sensitization.

Table 6
Lead optimization and lipophilicity values.

Ligands	cLogP	LE	LLE	LELP	Mutagenic
5a	3.662	0.413	4.774	8.885	High
5b	3.503	0.414	4.951	8.457	None
5c	3.318	0.413	4.774	8.885	None
5d	3.863	0.397	4.550	9.706	None
5e	4.412	0.382	3.942	11.54	None
5f	5.321	0.354	2.952	15.00	None
5g	5.775	0.342	2.462	16.86	None
5h	4.786	0.345	3.533	13.83	None
5i	4.667	0.346	3.663	13.47	None
5j	4.161	0.384	4.218	11.94	None
5k	4.405	0.347	3.951	12.68	None
5l	4.945	0.335	3.360	14.75	None

Table 7
Docking energy values of **5a–l** against butyrylcholinesterase.

Docking complexes	Binding Affinity(kcal/mol)
5a	−8.9
5b	−8.1
5c	−8.1
5d	−9.3
5e	−8.8
5f	−9.2
5g	−9.4
5h	−10.5
5i	−9.8
5j	−10
5k	−10.6
5l	−10.1

efficiency (LELP) values (Table 6). Prior research data showed that lipophilicity is a fundamental property to improve the lead structure efficacy and from lead candidate to drug development [37]. The lipophilicity of different compounds and predicted standard values for LE, LLE and LELP on the basis of cLogP value has been reported in data [38]. The proposed acceptable standard values were reported as for LE ($> \sim 0.30$ Kcal/mole/HA), LLE ($> \sim 5$ Kcal/mol), LELP ($-10 <$ to < 10) and cLogP (< 3), respectively. The predicted cLogP and LE values of our synthesized compounds results were comparable with standard values. The LLE predicted values showed that all generated values were in range with standard value LLE ($> \sim 5$ Kcal/mol). Moreover, LELP values of compounds (**5a–d**) were also approachable with the standard values while other showed little deviation with respect to standard value (Table 6). Furthermore, mutagenic effects was observed and predicted results showed that **5a** contains high mutagenic risk while all (**5b–l**) others did not showed any mutagenic effect.

3.4.6. Molecular docking and binding energy analyses

Molecular docking experiment is best approach to study the binding conformation of ligands within the active region of target proteins [39,40]. The docked complexes of synthesized compounds (**5a–l**) against BChE were analyzed on the basis of lowest binding energy values (kcal/mol) and hydrogen/hydrophobic interaction pattern. Results showed that all the ligands (**5a–l**) exhibited good docking energy values and showed their interaction within active region of target protein (Table 7). The docking energy values of all the docking complexes was calculated by using Eq. (i).

$$\Delta Gbinding = \Delta Ggauss + \Delta Grepulsion + \Delta Ghbond + \Delta Ghydrophobic + \Delta Gtors \quad \text{(i)}$$

Here, ΔG gauss: attractive term for dispersion of two gaussian functions, ΔGrepulsion: square of the distance if closer than a threshold value, ΔGhbond: ramp function - also used for interactions with metal ions, ΔGhydrophobic: ramp function, ΔGtors: proportional to the number of rotatable bonds. In docking energy results compounds selected as best having more than 2.5 kcal/mol energy value different compared to other compounds. The standard error for Autodock is reported as 2.5 kcal/mol (http://autodock.scripps.edu/;). Present docking results justified that the energy value difference among all docking complexes were lower than standard error value. Therefore, based on the basis of both *in vitro* and *in silico* docking energy results, **5c**, **5j** and **5k** was ranked as best ligands which showed good inhibitory potential against targeted enzyme as compared all other derivatives. Although, the basic nucleus of all the synthesized compounds were same, therefore most of compounds possess good efficient energy values and have no big energy fluctuations difference.

3.4.7. Binding pocket and ligands (5c, 5k and 5j) binding conformations

The binding pocket analysis showed that ligands (**5c, 5k** and **5j**) were confined in the active region of target protein. All three docked structures were superimposed to check their binding configuration in the active region of target protein. Results showed that these synthesized compounds were bound in the binding pocket having similar conformational pattern. Due to specific twisted geometry of **5c**, it was bound within the active region of target protein. Similarly, both **5j** and **5k** possessed particular tree dimensional orientation which allowed them to adjust their best conformational position inside the binding pocket of enzyme (Fig. 8).

3.4.8. Hydrogen and hydrophobic binding analysis

The docked complexes were analyzed on the basis of hydrogen and hydrophobic bonding interactions. The best in-vitro and docking energy result compounds (**5c, 5j** and **5k**) were selected to check their best conformational position inside active region of target protein (Fig. 9). The **5c** forms one hydrogen and one hydrophobic interactions at different residues within the active region of target protein. The piperazine ring of **5c** form π- π interaction against Tyr332 with bond length 4.75 Å. Similarly, the oxygen atom of 2-furyl part of **5c** forms a strong hydrogen bond against Pro285 having bonds distance 2.82 Å, respectively. Both hydrophobic and hydrogen bonding are in appropriate distances which give good stability to docking complex. Literature data also ensured the importance of these residues in bonding with other elastase inhibitors which strengthen our docking results. Eserine a standard drug used in *in vitro* analysis also formed H-bonds with Pro285 [41].

In **5j** docking complexes, one hydrophobic and two hydrogen bonds were observed with appropriate bonding distances. The piperazine ring of **5j** form π- π interaction against Tyr332 with bond length 5.27 Å. Similarly, the oxygen atom of 2-furyl part of **5j** forms a strong hydrogen bond against Trp82 having bonds distance 3.31 Å. Furthermore, the oxygen atom of sulfonyl group of **5j** from hydrogen bond against Thr120 having bond length 2.26 Å. The hydrogen and hydrophobic interactions strengthen the conformation of ligand within the active region of target protein. Prior computational data results also support our docking results and same residues are involve in binding interaction [42,43].

In **5k** docking complexes, single hydrophobic and two hydrogen bonds were observed with suitable bonding distances. The 2-furyl ring part of **5k** forms a hydrophobic interaction against aromatic Trp82 having bonds distance 4.86 Å. Furthermore, the oxygen atom of sulfonyl group of **5k** from hydrogen bond against Thr120 having bond length 2.85 Å. The chlorine atom at ortho position in the benzene structure is also involved hydrogen bond with bond distance 2.85 Å). The comparative results showed that all docking results depicted some common residues which strengthen our docking efficacy and

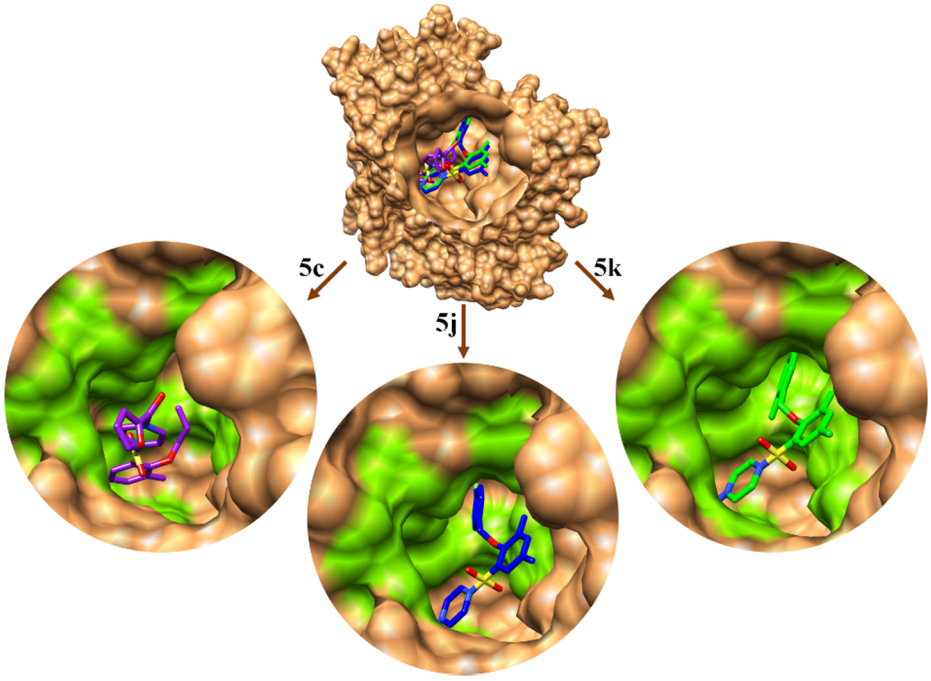

Fig. 8. Binding pocket conformation of **5c**, **5j** and **5k** in the target protein.

credibility. Moreover, the already published computational data results also showed good correlation with our docking results [42,43]. The 2-dimensional graphical depiction of remaining complexes is mentioned in Supplementary data (Figs. S2–S10).

3.4.9. Root mean square deviation and fluctuation analysis through MD simulation

Based on *in vitro* and docking results, **5c** and **5j**-BChE complexes were selected for dynamic simulation analysis using Gromacs 4.5.4 tool.

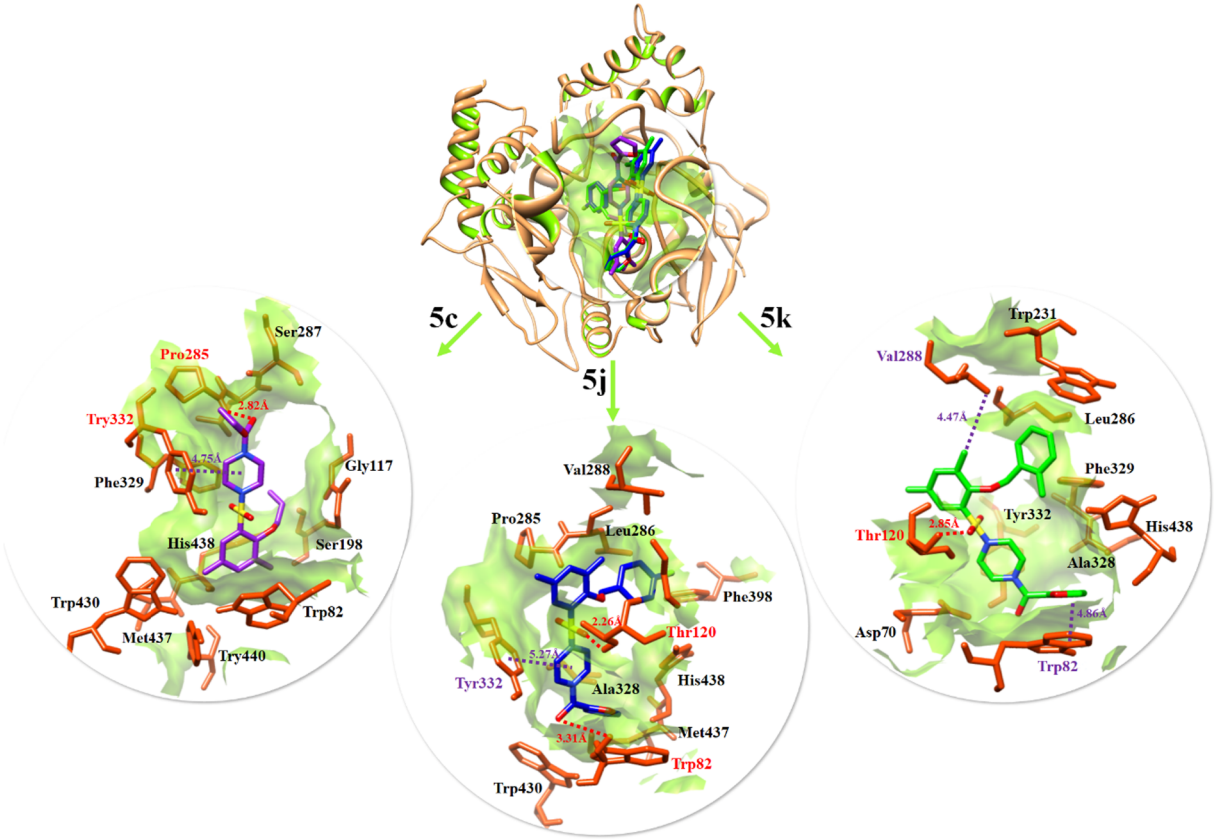

Fig. 9. Docking complexes of **5c, 5j** and **5k.** The ligand structures **5c**, **5j** and **5k** are highlighted in purple, blue and green colors while the interactive residues are depicted in brown color. The protein structure is justified in green color in surface format and binding distances are represented in purple and red dotted lines in angstrom Å.

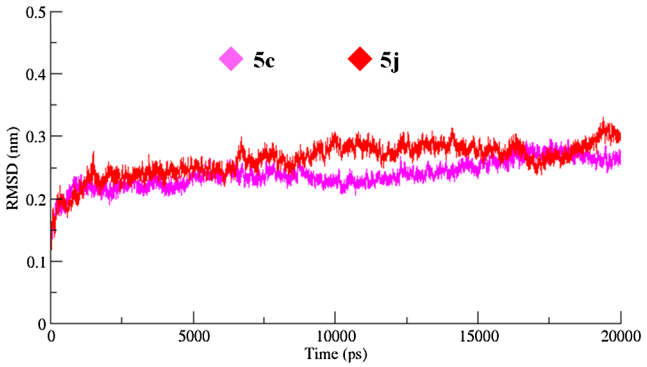

Fig. 10. RMSD graph of all the docking structures from 0 to 20,000 ps simulation time frame.

The protein backbone structural fluctuated behavior were examined by generating RMSD and RMSF graphs. The RMSD results showed that protein backbone deviation and fluctuations behavior in the simulation time frame from 0 to 20,000 ps. Both pink (**5c**) and red (**5j**) graph lines depicted good stable and steady results with little fluctuated behavior in simulation time period. Initially, both graphs lines showed their fluctuations with RMSD value range form 0.1–0.2 nm from simulation time 0–2500 ps. From time 2500–7500 ps both complexes remain stable and no big fluctuations were observed in it and their RMSD values remain stable 0.25 nm. The little increasing trend was observed in RMSD graph line (red) form 7500 to 15,000 ps having RMSD value 0.35 nm. Whereas, the pink graph line (**5c**) showed its stability compared to red graph line (**5j**) in the same time period (7500–15,000 ps). However, from 15,000 to 20,000 ps the **5j** complex showed high fluctuations whereas, **5c** remain steadily stable in the simulation time period. The comparative analysis showed that **5c** complex remain more stable as compared to **5j** (Fig. 10). The RMSF results of all three docking protein structures dynamically fluctuated from residues N to C terminals. The RMSF results of **5c** and **5j**-docking structure dynamically fluctuated from residues N to C terminals. Little fluctuation peaks within loops region were observed at *N*-terminus region while higher peaks were observed at C-terminal (Fig. 11).

3.4.10. Radius of gyration and solvent accessible surface area analyses

The structural compactness in protein docking complexes were observed by radius of gyration (Rg). The stably folded proteins show the relatively steady value of Rg, whereas the disturbed regions of proteins show higher fluctuations in Rg values in the simulation time period (0–20,000 ps). The generated results depicted that Rg value of both complexes remain sable with Rg value 2.225 nm. However, minute

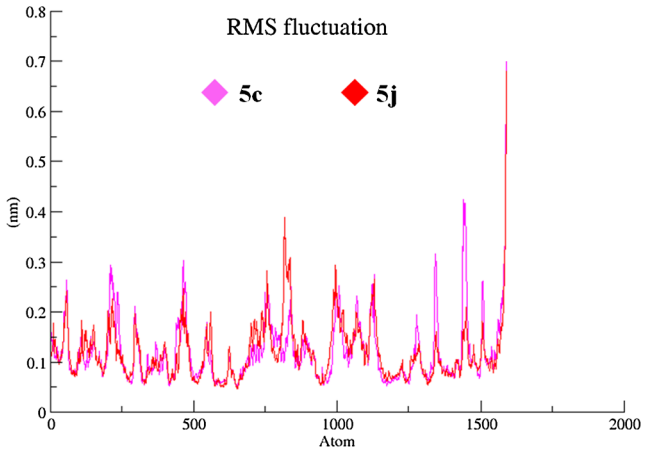

Fig. 11. RMSF graph of **5c** and **5j** docking structures from 0 to 20,000 ps simulation time frame.

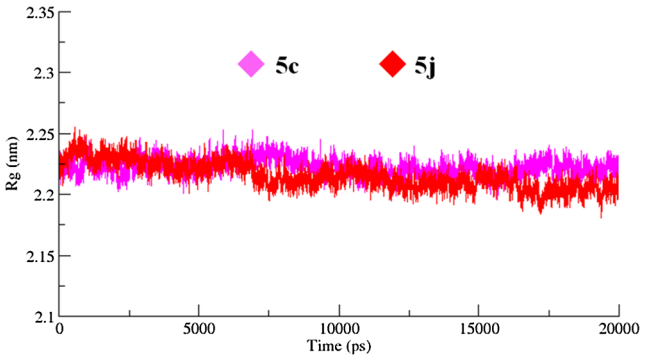

Fig. 12. Rg graph of **5c** and **5j** docking structures from 0 to 20,000 ps simulation time frame.

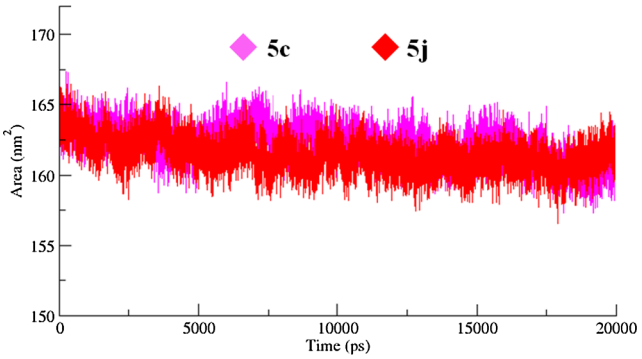

Fig. 13. SASA graph of **5c** and **5j** docking structures from 0 to 20,000 ps simulation time frame.

fluctuations were seen in both (**5c** and **5j**) structures from 0 to 20,000 ps simulation time. (Fig. 12).

The solvent-accessible surface areas (SASA) were also observed and shown in (Fig. 13). Results showed that the SASA values of both **5c** and **5j**-docking complexes were centered on 162.5 nm^2 in the simulation time 0–20,000 ps. The generated energy graph showed that both complexes were attained stable energy value in the simulation time period 0–20,000 ps (Fig. 14).

4. Conclusion

In conclusion, we discovered that some 2-furyol piperazine containing sulfonamides behaved as promising inhibitors of BChE. The compounds **5c**, **5j** and **5k** exhibited noteworthy inhibitory potentials with IC_{50} values of 9.51 ± 0.06, 17.69 ± 0.07 and 15.43 ± 0.09 μM, respectively. Hence, these three compounds can serve as suitable chemical templates for the designing of new medicinal scaffolds for the treatment of Alzheimer's disease.

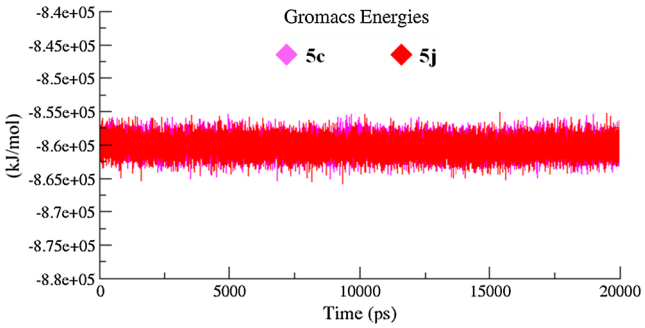

Fig. 14. Energy graph of **5c** and **5j** docking structures from 0 to 20,000 ps simulation time frame.

Appendix A. Supplementary material

Supplementary data to this article can be found online at https://doi.org/10.1016/j.bioorg.2019.103138.

References

[1] M.A. Abbasi, M. Islam, Aziz-ur-Rehman, et al., Synthesis, characterization, antibacterial, α-glucosidase inhibition and hemolytic studies on some new n-(2,3-Dimethylphenyl)benzenesulfonamide derivatives, Trop. J. Pharm. Res. 15 (2016) 591–598.

[2] C.T. Supuran, A. Casini, A. Scozzafava, Protease inhibitors of the sulfonamide type: anticancer, antiinflammatory, and antiviral agents, Med. Res. Rev. 23 (2003) 535–558.

[3] G. Hussain, M.A. Abbasi, Aziz-ur-Rehman, et al., Synthesis and molecular docking study of some new 4-{[4-(2-furoyl)-1-piperazinyl]methyl}-N-(substituted-phenyl) benzamides as possible therapeutic entrants for Alzheimer's disease, Med. Chem. (Los Angeles) 6 (2016) 129–136.

[4] N. Öztaşkın, R. Kaya, A. Maraş, E. Şahin, İ. Gülcin, S. Göksu, Synthesis and characterization of novel bromophenols: determination of their anticholinergic, antidiabetic and antioxidant activities, Bioorg. Chem. 87 (Jun) (2019) 91–102.

[5] H. Genç Bilgiçli, A. Kestane, P. Taslimi, O. Karabay, A. Bytyqi-Damoni, M. Zengin, İ. Gulçin, Novel eugenol bearing oxypropanolamines: synthesis, characterization, antibacterial, antidiabetic, and anticholinergic potentials, Bioorg. Chem. 88 (Jul) (2019) 102931.

[6] M. Boztas, P. Taslimi, M.A. Yavari, I. Gulcin, E. Sahin, A. Menzek, Synthesis and biological evaluation of bromophenol derivatives with cyclopropyl moiety: ring opening of cyclopropane with monoester, Bioorg. Chem. 28 (89) (2019) 103017.

[7] U. Atmaca, R. Kaya, H.S. Karaman, M. Çelik, İ. Gülçin, Synthesis of oxazolidinone from enantiomerically enriched allylic alcohols and determination of their molecular docking and biologic activities, Bioorg. Chem. 88 (2019 Jul) 102980.

[8] K.R. Varadaraju, J.R. Kumar, L. Mallesha, et al., Virtual screening and biological evaluation of piperazine derivatives as human acetylcholinesterase inhibitors, Int. J. Alzheimers. Dis. 2013 (2013) 653962.

[9] P. Meena, V. Nemaysh, M. Khatri, et al., Synthesis, biological evaluation and molecular docking study of novel piperidine and piperazine derivatives as multi-targeted agents to treat Alzheimer's disease, Bioorg. Med. Chem. 23 (2015) 1135–1148.

[10] N.H. Greig, D.K. Lahiri, K. Sambamurti, Butyrylcholinesterase: an important new target in Alzheimer's disease therapy, Int. Psychogeriatr. 1 (2002) 77–91.

[11] M. Mesulam, A. Guillozet, P. Shaw, et al., Widely spread butyrylcholinesterase can hydrolyze acetylcholine in the normal and Alzheimer brain, Neurobiol. Dis. 9 (2002) 88–93.

[12] S. Diamant, E. Podoly, A. Friedler, et al., Butyrylcholinesterase attenuates amyloid fibril formation in vitro, Proc. Natl. Acad. Sci. USA 103 (2006) 8628–8633.

[13] E.K. Perry, R.H. Perry, G. Blessed, et al., Changes in brain cholinesterases in senile dementia of Alzheimer type, Neuropathol. Appl. Neurobiol. 4 (1978) 273–277.

[14] A. Nordberg, C. Ballard, R. Bullock, et al., A review of butyrylcholinesterase as a therapeutic target in the treatment of Alzheimer's disease, Prim. Care Compan. CNS Disord. 15 (2013) PCC.12r01412.

[15] P. Davies, A.J. Maloney, Selective loss of central cholinergic neurons in Alzheimer's disease, Lancet 2 (1976) 1403.

[16] G.L. Ellman, K.D. Courtney, V. Andres, et al., A new and rapid calorimetric determination of acetylcholinesterase activity, Biochem. Pharmacol. 7 (1961) 88.

[17] P. Sharma, J.D. Sharma, In vitro hemolysis of human erythrocytes by plant extracts with antiplasmodial activity, J. Ethnopharmaco. 74 (2001) 239.

[18] W.A. Powell, C.M. Catranis, C.A. Maynard, Design of self-processing antimicrobial peptide for plant protection, Lett. Appl. Microbiol. 31 (2000) 163.

[19] F. Nachon, E. Carletti, C. Ronco, et al., Crystal structures of human cholinesterases in complex with huprine W and tacrine: elements of specificity for anti-Alzheimer's drugs targeting acetyl- and butyryl-cholinesterase, Biochem. J. 453 (2013) 393–399.

[20] E.F. Pettersen, T.D. Goddard, C.C. Huang, et al., UCSF chimera – a visualization system for exploratory research and analysis, J. Comput. Chem. 25 (2004) 1605–1612.

[21] L. Willard, A. Ranjan, H. Zhang, et al., VADAR: a web server for quantitative evaluation of protein structure quality, Nucl. Acids Res. 31 (2003) 3316–3319.

[22] Studio Discovery, "version 2.1.", Accelrys, San Diego, CA, 2008.

[23] D.E. Pires, T.L. Blundell, D.B. Ascher, pkCSM: predicting small-molecule pharmacokinetic properties using graph-based signatures, J. Med. Chem. 58 (2015) 4066–4072.

[24] T. Sander, J. Freyss, M. von Korff, et al., DataWarrior: an open-source program for chemistry aware data visualization and analysis, J. Chem. Inf. Model. 55 (2015) 460–473.

[25] S. Dallakyan, A.J. Olson, Small-molecule library screening by docking with PyRx, Meth. Mol. Biol. 1263 (2015) 243–250.

[26] S. Pronk, S. Páll, R. Schulz, et al., GROMACS 4.5: a high-throughput and highly parallel open source molecular simulation toolkit, Bioinformatics 29 (2013) 845–854.

[27] S.W. Chiu, S.A. Pandit, H.L. Scott, et al., An improved united atom force field for simulation of mixed lipid bilayers, J. Phys. Chem. B 113 (2009) 2748–2763.

[28] H. Wang, F. Dommert, C. Holm, Optimizing working parameters of the smooth particle mesh Ewald algorithm in terms of accuracy and efficiency, J. Chem. Phys. 133 (2010) 034117.

[29] S. Amiri, M.S. Sansom, P.C. Biggin, Molecular dynamics studies of AChBP with nicotine and carbamylcholine: the role of water in the binding pocket, Protein Eng. Des. Sel. 20 (2007) 353–359.

[30] D.F. Veber, S.R. Johnson, H.Y. Cheng, et al., Molecular properties that influence the oral bioavailability of drug candidates, J. Med. Chem. 45 (2002) 2615–2623.

[32] M.A. Bakht, M.S. Yar, S.G. Abdel-Hamid, et al., Molecular properties prediction, synthesis and antimicrobial activity of some newer oxadiazole derivatives, Eur. J. Med. Chem. 45 (2010) 5862–5869.

[33] S. Tian, J. Wang, Y. Li, et al., The application of in silico drug-likeness predictions in pharmaceutical research, Adv. Drug Deliv. Rev. 86 (2015) 2–10.

[34] W.P. Walters, Ajay, M.A. Murcko, Recognizing molecules with drug-like properties, Curr. Opin. Chem. Biol. 3 (1999) 384–387.

[35] A. Husain, A. Ahmad, S.A. Khan, et al., Synthesis, molecular properties, toxicity and biological evaluation of some new substituted imidazolidine derivatives in search of potent anti-inflammatory agents, Saudi Pharm. J. 24 (2016) 104–114.

[36] K. Mortelmans, E. Zeiger, The Ames Salmonella/microsome mutagenicity assay, Mutat. Res. 455 (2000) 29–60.

[37] T.I. Oprea, A.M. Davis, Teague SJ. Et, et al., Is there a difference between leads and drugs? A historical perspective, J. Chem. Inf. Comput. Sci. 41 (2001) 1308–1315.

[38] A.L. Hopkins, G.M. Keserü, P.D. Leeson, et al., The role of ligand efficiency metrics in drug discovery, Nat. Rev. Drug Discov. 13 (2014) 105–121.

[39] M. Hassan, S. Shahzadi, S.Y. Seo, et al., Molecular docking and dynamic simulation of AZD3293 and solanezumab effects against BACE1 to treat Alzheimer's disease, Front. Comput. Neurosci. 12 (2018) 34.

[40] M.A. Abbasi, M. Hassan, Aziz-Ur-Rehman, et al., Synthesis, enzyme inhibitory kinetics mechanism and computational study of N-(4-methoxyphenethyl)-N-(substituted)-4-methylbenzenesulfonamides as novel therapeutic agents for Alzheimer's disease, PeerJ 6 (2018) e4962.

[41] M. Lateef, A.A.B. Siddiqui, S. Zarina, et al., New anthrarobin acyl derivatives as butyrylcholinesterase inhibitors: synthesis, in vitro and in silico studies, Heliyon 3 (2017) e00350.

[42] K. Lodarski, J. Jończyk, N. Guzior, et al., Discovery of butyrylcholinesterase inhibitors among derivatives of azaphenothiazines, J. Enzyme Inhib. Med. Chem. 30 (2015) 98–106.

[43] A. Kostelnik, M. Pohank, Inhibition of acetylcholinesterase and butyrylcholinesterase by a plant secondary metabolite boldine, Biomed Res. Int. 2018 (2018) 9634349.